Materials Research Proceedings 41 (2024) 2658-2667 https://doi.org/10.21741/9781644903131-291

Rheological behavior of nanofillers enclosed multilayer systems under elongational flows: From microlayers to nanolayers

LI Jixiang[1,a], MAAZOUZ Abderrahim[1,b] and LAMNAWAR Khalid[1,c*]

[1]Université de Lyon, CNRS, UMR 5223, Ingénierie des Matériaux Polymères, INSA Lyon, F-69621, Villeurbanne, France

[a]jixiang.li@insa-lyon.fr, [b]abderrahim.maazouz@insa-lyon.fr, [c]khalid.lamnawar@insa-lyon.fr

Keywords: Polymer Nanocomposites, Multilayer, Forced Assembly, Elongational Flow

Abstract. The present work dedicated in the elongational behavior of multilayer polymer nanocomposites. CNTs were enclosed in a polypropylene with linear chain structure (PPC) and then co-extruded with another polypropylene (PPH) with long chain branching (LCB). By forced assembly, multilayer films with layer thickness from micro to nano were fabricated and the elongational rheology test was then conducted with the extension vertical to the film extrusion direction. Due to the LCB inside PPH, all multilayer films showed obvious strain hardening behavior despite linear PPC is a strain softening polymer. When the layer numbers were fewer, namely, the layer thickness was higher than the length of the CNTs, the strain hardening behavior of nanocomposite films was close to the multilayer system with neat polymers. With the layer numbers increasing, the layer thickness became lower than the length of the CNTs and the strain hardening behavior of nanocomposite films increased dramatically compared to the multilayer system with neat polymers. The reason for this kind behavior was because of the better orientation of CNTs via layer confinement when layer numbers increased, which thus making the strain hardening more significant.

Introduction

With the coming era of 5G, the demand of materials with higher efficiency for electromagnetic interference (EMI) shielding is growing rapidly. Enclosing conductive fillers into multilayer polymer films has been reported to enhance the EMI shielding properties dramatically[1–3]. Popular techniques of fabricating Multilayer films including layer-by-layer casting, spin coating or compression molding are often with many steps and hard to be industrialized[4]. Therefore, forced assembly co-extrusion seems to be a better solution for this problem as the process is continuous. During the forced assembly, the flow effects to the fillers dispersion and alignment can be crucial for the final properties.

Extensional rheology is a rapid developing technology[5] to study multilayer systems recently which can reflect chain entanglement in the interphase as well as interfacial slip and failure dramatically[6] . For example, Zhang et al. created a compatible multilayer film by combining poly(methyl methacrylate) (PMMA)and poly(vinylidene fluoride) (PVDF) with a composition of 50% using layer-multiplying coextrusion[7]. Besides, elongational rheology also can be effective to detect the nanofillers behavior during melt state, which is rarely been studied.

In this context, polypropylenes with chain structure of linear (PPC) and long chain branching (PPH) were applied as the polymer pair for co-extrusion and carbon nanotubes (CNTs) as the conductive fillers enclosed in PPC. Multilayer films with different layer numbers from micro-layer to nano-layer thickness were fabricated. Extension rheology was then conducted to investigate the strain hardening behavior of PPH/PPC(CNTs) films and compared with PPH/PPC films and Neat polymers to reflect the fillers alignment during forced assembly co-extrusion.

Experiment section

Materials: PPC (polypropylene, RD204CF, Borealis AG, Austria) and PPH (polypropylene, Daploy™ WB140HMS, Borealis AG, Austria) were chosen as the polymer matrices. The melt flow rate (MFR) of PPC was 8 g/10min and that of PPH was 2.1 g/10min. Multiwall Carbon Nanotubes (CNTs) were purchased from Nanocyl SA in Belgium and their properties are listed in Table 1.

Table 1 Physical properties of the CNTs

Diameter (nm)	Average length (μm)	Surface Area (m^2/g)
7~20	1.5	250~300

Sample preparation: The CNTs were melt mixed with PPC in a twin-screw extruder to prepare masterbatches with a CNT amount of 2 wt% (PPC(CNTs)). PPH and PPC(CNTs) with volume fraction of 50/50 were then co-extruded via a homemade multilayer coextrusion setup as schemed in Figure 1. Two extruders were combined through a feedblock from where a series of layer multiplication dies were connected. The two different polymer melts first meet in the feedblock in a bilayer configuration, then, when going through the layer multiplication dies, the melt is successively split vertically and horizontally spread back to its original width before being stacked again, keeping the total film thickness constant. The final number of layers is determined by the number of multipliers used. During the coextrusion process, the melt temperature was set at 260°C for the extruders, multipliers, and die. The chill-roll temperature was set to 90°C and at certain speed to obtain a total film thickness of 500±50 μm. The stretching ratio was kept low as the focus is mainly set on the structuration due to the coextrusion and layer multiplication processes rather than chain orientation by drawing. The feedblock configuration used for the systems was a A/B/A configuration, where A and B correspond to the extruders displayed in Figure 1. A set of N multipliers leads to a final film of 2N+1 +1 layers. Neat PPH and PPC were also co-extruded as references. Multilayer films of neat PPH and PPC with volume fraction of 50/50 were also prepared similarly via the coextrusion setup as references. Besides, Neat polymers, the 50/50 volume fraction blend films of PPH/PPC and PPH/ PPC(CNTs) were also extruded by the setup where only extruder A was using.

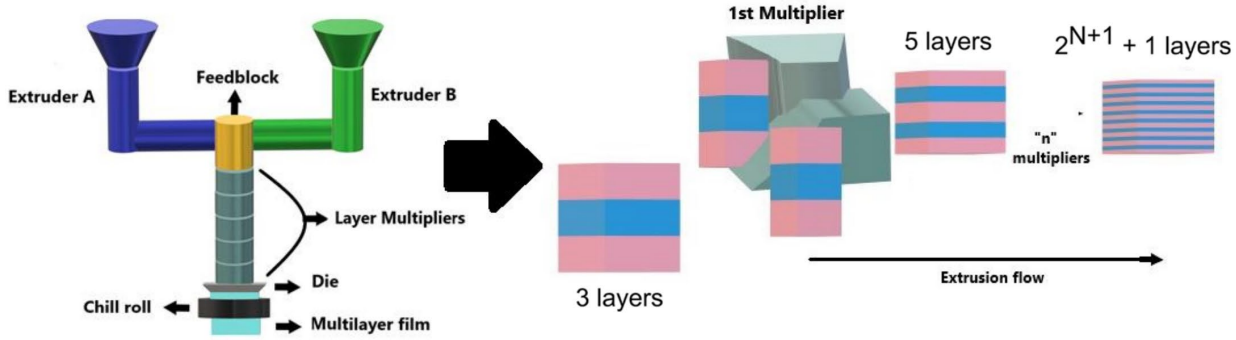

Figure 1 Schematic illustration of layer multiplication in the homemade multilayer coextrusion setup.

All produced and studied multilayer films are listed in Table 2 with PPH combined with PPC or PPC(CNTs), where n is the number of multipliers and N the corresponding number of layers. The estimated nominal layer thickness for each layer with a A/B film configuration was calculated using Equation 1.

$$h_{nomA,B} = \varphi_{A,B} \frac{h_{total}}{2^n} \quad (1)$$

where φ_A and φ_B represent the volume fraction of A and B, respectively, $h_{total}$the total film thickness and n the number of multipliers.

Table 2. Characteristics of the multilayered PPH/PPC and PPH/PPC(CNTs) films, where the h_T represent the total thickness of the film and h_N represent the thersitical layer thickness.

Polymer systems		PPH/PPC		PPH/PPC(CNTs)	
no. of layers (*N*)	no. of multipliers (*n*)	h_T (μm)	h_N	h_T (μm)	h_N
3L	0	518	259 μm	530	265 μm
17L	3	524	32.75 μm	541	33.81 μm
257L	6	486	1.89 μm	492	1.92 μm
1025L	9	526	510 nm	515	500 nm

Size exclusion chromatography and multi-angle laser light scattering (SEC-MALLS): The average molecular weights and the polymer chain microstructure were determined by SEC-MALLS which is a combination of SEC for separation with a multi-angle laser scattering (MALLS) for analysis. Both PP samples were run at 160°C with 1,2,4- trichlorobenzene (TCB) as the solvent and at a flow rate of 1 mL/ min. The light scattering detector was placed in line between the SEC system and the refractive index detector. The absolute molecular weight and radius of gyration Rg of both PPs used in this study were measured directly by the SEC-MALS technique, and as a result the long-chain branching distribution and content in the PPs could be determined by direct application of the Zimm–Stock approach[8].

Uniaxial Extensional Rheology: Uniaxial extensional rheology was carried out using a Sentmanat extensional rheometer fixture (SER-2, Xpansion Instruments, LLC) mounted on the DHR-2 rheometer.29,36 Samples from the extrusion process were cut into rectangular strips with the following dimensions: length, width, and thickness of 20 mm × 10 mm × 0.5 mm (width along the extrusion direction) for the extensional test. Each sample was preheated at the tested temperature for 120 s in the rheometer oven before tests and was observed with a built-in camera to ensure sagging did not occur. Extensional flow data were then collected with extension vertical to the film extrusion direction at a constant Hencky strain rate at 180 °C under nitrogen. All measurements were repeated at least three times.

Results and discussion

The combination of SEC and MALLS is a versatile and reliable means of characterizing the polymer chain microstructure. In this study, the LCBs of PPH could be clearly reflected by analysis of the SEC-MALLS results. The molar mass distributions and radius of gyration (R_g) related to the molar mass of the two polymers are illustrated in Figure 2. The broader distribution of the molecular weight with two peaks of PPH was the first clue to the presence of LCBs. Meanwhile, the nonlinearity of R_g for PPH related to molar mass also suggested a disparate polymer chain microstructure between PPC and PPH.

For PPC with linear chain structure, the curve of log R_g complied well with the linear reference of linear PP[9]. On the other hand, higher values of R_g of the lower molecular weight PPH and a deviation from the linear reference PP curve in the higher molecular area indicated a probable branched or star-like chain structure in PPH[10]. This last feature is typical of LDPE and has also been found for electron beam irradiated polypropylenes[11,12].

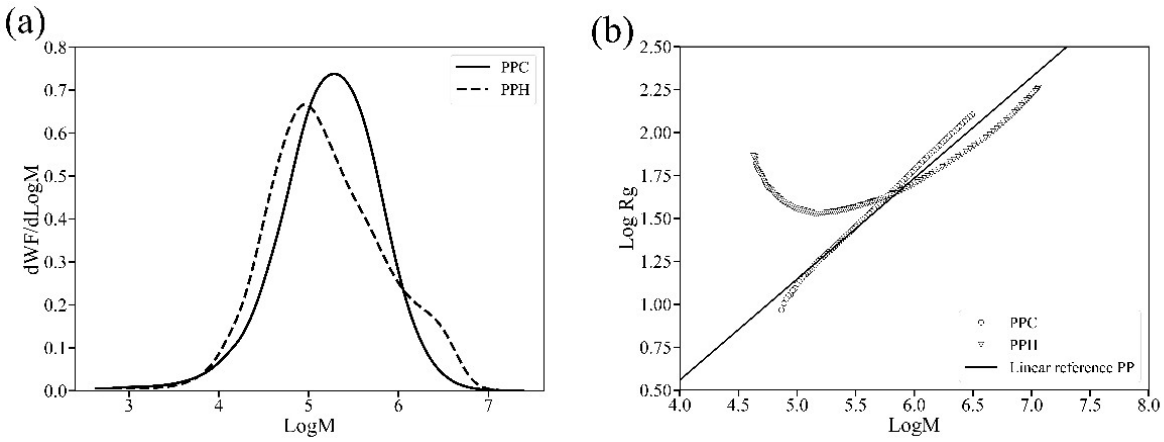

Figure 2 Size exclusion chromatography traces of the studied PP samples.

More concrete evidence can be obtained by calculating the viscosity branching index g', the average number of branched points B_n and the LCB frequency λ. The values of B_n and λ between molecular weights of 3×10^4 and 1×10^6 g/mol are listed in Table 3. Although no great amount of LCBs was detected in PPH, there was already a significant influence on the viscoelastic properties compared with PPC with a linear chain structure.

Table 3 Long-chain branching characteristics. Viscosity branching index, average LCB per molecule and average branching frequency per 1000 units for PPH between 3×10^4 *and* 1×10^6 *g/mol.*

	g'	B_n (LCB/molecule)	λ (LCB/1000 monomers)
PPH	0.67	1.73	1.50

The extensional viscosities, η_E^+, of PPC and PPH melts as functions of time at constant Hencky strain rates, $\dot{\varepsilon}_H$, ranging from 0.3 S^{-1} to 10 S^{-1}, are presented in Figure 3. The linear viscoelastic (LVE) curves which corresponded very well with the threefold value of the linear viscosity ($3\eta_0^+$) [13] measured during startup shear in the range of linear deformation are also displayed. Apparently, PPC with linear chain structure is a strain softning polymer with very slight strain hardening observed at the $\dot{\varepsilon}_H$ of 10 S^{-1} ,which complies with other report[14]. By contrast, the phenomena that occurred for PPH were different. For all $\dot{\varepsilon}_H$ tested in this work, the PPH samples showed obvious strain hardening behaviors. In fact, polymers with LCB resisted chain disentanglement[15], particularly in extension, wherefore the final collapse of the entanglement network was effectively postponed. Such behavior would be favorable for stable film blowing and fiber spinning. In summary, it can be suggested that the presence of LCB in PPH favored the more obvious strain hardening behaviors during the elongational experiments. In contrast, PPC with its linear structure showed less strain hardening.

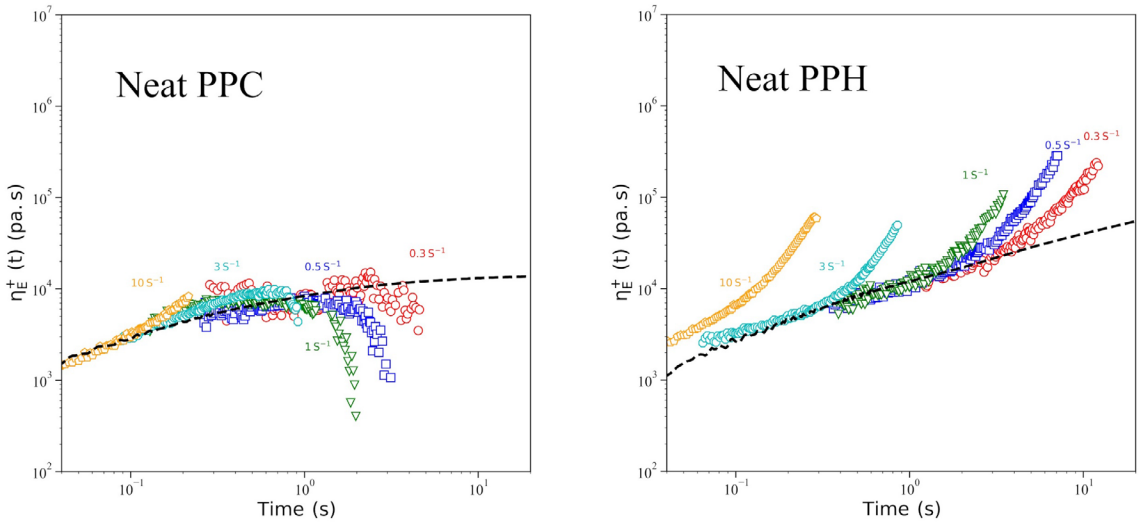

Figure 3 Elongation viscosity vs time at (a) 180 °C in startup uniaxial extension with constant Hencky strain rates ranging from 0.3 to 10.0 s^{-1} for PPC and PPH

The extensional viscosities of multilayer films with layer numbers of 17L and 1025L are shown in Figure 4. To clearer manifesting the tendency and comparing, extensional curves with $\dot{\varepsilon}_H$ of only 0.3 S^{-1} were presented. Blend and neat polymer films are also displayed as references. It can be suggested that except Neat PPC, all other films show strain hardening behavior indicating its sensitivity to the LCB[10,16]. Negative deviation of blend film curve with CNTs (CNTBlend) from neat polymer blend (Neat Blend) curve manifest the decrease of strain hardening due to the CNTs loading. The nanoparticles influence to the strain hardening behavior under elongational flow is reported to be complicated and may be related to the size, dispersion and attractive force between nanoparticles[17]. With the increased amounts of nanoparticles, the elongation viscosity often increased at lower $\dot{\varepsilon}_H$ [18,19]. However, the strain hardening behavior at higher Hencky strain may disappeared or decreased. Elongation thinning may even happen at high $\dot{\varepsilon}_H$ [20]. This is because at higher nanoparticles loading, especially higher than the percolation threshold, the aggregation of nanofillers form a rigid network making the film melt more solid like thus without extensibility[19]. In contrast, lower quantity of well dispersed nanofillers show less significant influence on the extensional viscosities of the system. In some cases, increased strain hardening may occur when enhancing the interaction between nano fillers and polymer chains[17]. Whereas, poor dispersed nanofillers inside the polymer matrix will lead to the disappear or decrease of strain hardening. In our blend cases, the CNTs were first dispersed in PPC and then mixed with PPH inside a single-screw extruder where the shear force is comparatively lower and the weight percentage of CNTs were only 1 wt%. Therefore, the dispersion of CNTs inside the blend films were not very well and these unconnected aggregates of CNTs may be the reason for the decrease of strain hardening compare to the neat polymer blend films.

For the multilayer films with neat polymers, the elongation viscosities are highly depended on the polymer pair properties and the number of layers, which were carefully studied by our previous work[21–23]. Generally, for multilayer system with two different polymers, a simple additivity rule can be applied to predict the elongational viscosity according to the elongational viscosities of the two neat polymers. Upon the uniaxial extension, the deformation rate for each layer in the multilayer structure is the same. The total force is the sum of the contributions of constituent layers and interphase/interlayer, which could be estimated with the following equation (2):

$$F(t) = \sigma_A A_A(t) + \sigma_B A_B(t) + \sigma_{int} A_{int}(t) \quad (2)$$

where $\sigma_i(t)$ is the Cauchy stress of layer i (i denotes component layer A, B and the interphase/interlayer). $A_i(t)$ is the area of cross section parallel to the film coextrusion direction with $A_i(t) = W_i(t) \times H_i(t)$, where $W_i(t)$ and $H_i(t)$ are the time-dependent width and thickness of a layer i, respectively. Therefore, the transient extensional viscosity of the total multilayer structure including interphases can be described as:

$$\eta_E^+(t) = \frac{F(t)}{\dot{\varepsilon}A(t)} = \phi_A \frac{\sigma_A(t)}{\dot{\varepsilon}} + \phi_B \frac{\sigma_B(t)}{\dot{\varepsilon}} + \phi_{int} \frac{\sigma_{int}(t)}{\dot{\varepsilon}} = \phi_A \eta_{E,A}^+(t) + \phi_B \eta_{E,B}^+(t) + \phi_{int} \eta_{E,int}^+(t) \quad (3)$$

in which $\phi_i$is the volume fraction of layer i with $\phi_i = {A_i(t)}/{A_{total}(t)} = {H_i(t)}/{H_{total}(t)}$. Specifically, in the absence of an interphase layer, eq (4) can be simplified to rule as follows[24]:

$$\eta_E^+(t) = \phi_A \eta_{E,A}^+(t) + \phi_B \eta_{E,B}^+(t) \quad (4)$$

During forced assembly, when the layer numbers are fewer, the contact time in the multiplier elements is less and the experimental data of elongational viscosity curve usually follows the prediction of additivity rule. When the layer numbers increased, the contact time increased with the numbers of multipliers. If the two polymers are miscible, interfacial diffusion would happen in case of films with high number of layers and would cause a positive deviation of experimental elongational viscosity curve from the simple additivity rule in absence of an interphase layer, which has been addressed in the study related to the multilayer system of PVDF and PMMA[22,23]. This is because of the increased chain entanglement between polymer-polymer interface. In addition, this kind of phenomenon may also happen when the polymer pairs are immiscible[25]. In our cases, as the polymer pairs are the same polymer with different chain structures, they are totally miscible thus causing the positive deviation of almost all the multilayer films from the calculated additivity rule using neat PPC and PPH (as the solid line shown in Figure 4 (a) and (b)). Therefore, the extensional behaviors of multilayer systems with neat PPC and PPH are close to the PPC/PPH blend films.

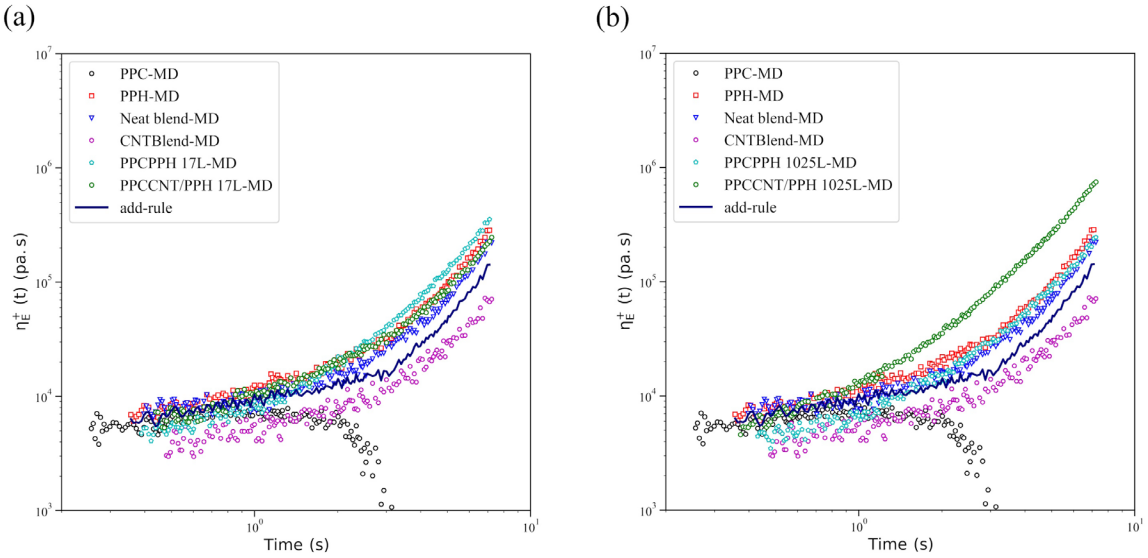

Figure 4 Elongation viscosity vs time at 180 °C with constant Hencky strain rates of 0.5 s^{-1} of neat polymer, blend and multilayer films where (a) 17L and (b) 1025L. All films were tested in the direction vertical to the extrusion direction. Solid line were calculated from additivity rule.

When adding CNTs into the PPC layer, the influence to the elongational viscosity of multilayer system with 17L was less significant as shown in Figure 4(a). Only a slight decrease of strain hardening was observed which is reasonable as the CNTs weight percentage was only 1 wt%. Conversely, when the layer number reached 1025, the strain hardening of multilayer system with CNTs was apparently enhanced compared with the film without CNTs. As the CNTs weight percentage was still 1wt%, we assumed to regard this phenomenon to the orientation of CNTs due to the layer confinement by PPH. In our previous work, we got the evidence that CNTs mobility inside a LCB polymer is restricted[26]. Therefore, during the forced assembly, CNTs are more pronounced to move with the flow inside PPC layer. With layer numbers increased, the nominal thickness of PPC layer decreased dramatically blow the length of CNTs as shown in Table 2 and the CNTs would be confined by the PPH layer causing a better orientation parallel to the extrusion direction as well as the layer interface as shown in Figure 5. As our extension direction was perpendicular to the extrusion direction, namely, it was also perpendicular to the CNTs orientation direction. The enhanced strain hardening is because of the increased force to change the CNTs orientation during stretching. The influence of strain hardening from the fillers orientation by flow was also reported by Yu wei et al where their tested fillers are glass fibers[27]. In our cases, it is the coordination of flow and layer confinement that enhanced the orientation of CNTs as well as the strain hardening of the loading films.

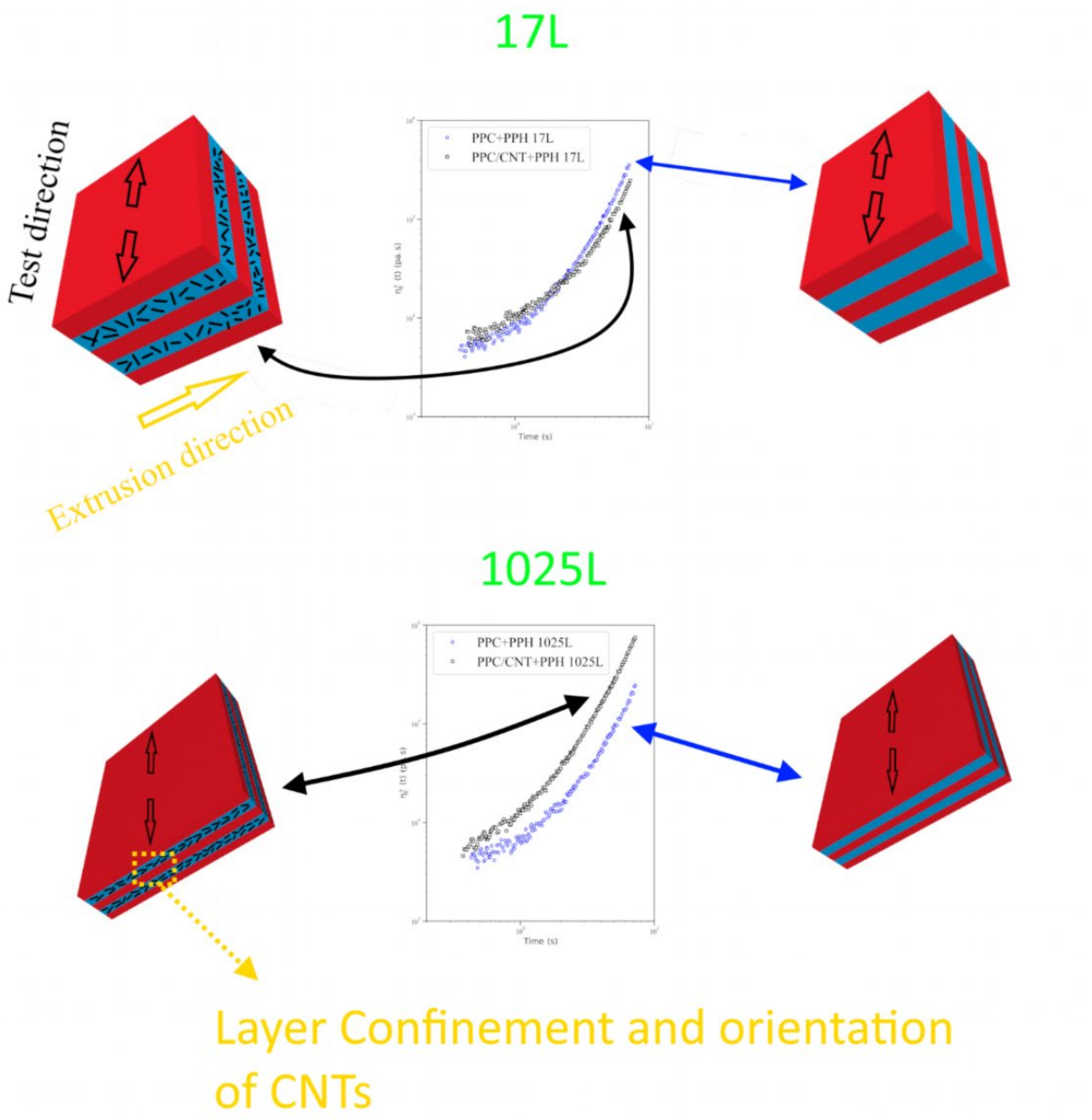

Figure 5 Proposed schematic illustration displaying the increased strain hardening due to the CNTs orientation caused by layer confinement with layer numbers increased.

Conclusions

In summary, the elongation behaviors of polymer nanocomposites with multilayer structure were revealed in this work. Both blend films and multilayer films showed strain hardening behavior because of the LCB inside PPH, even though PPC alone was a strain softening polymer. The small amount of CNTs inside the films cause less significant influence to the films with fewer number of layers but strongly enhanced strain hardening to the films with a greater number of layers due to the better CNTs orientation which was beneficial from the coordination of extrusion flow and layer confinement.

References

[1] B. Zhou, Z. Zhang, Y. Li, G. Han, Y. Feng, B. Wang, D. Zhang, J. Ma, C. Liu, Flexible, Robust, and Multifunctional Electromagnetic Interference Shielding Film with Alternating Cellulose Nanofiber and MXene Layers, ACS Appl. Mater. Interfaces 12 (2020) 4895–4905. https://doi.org/10.1021/acsami.9b19768

[2] G. Yin, Y. Wang, W. Wang, D. Yu, Multilayer structured PANI/MXene/CF fabric for electromagnetic interference shielding constructed by layer-by-layer strategy, Colloids and Surfaces A: Physicochemical and Engineering Aspects 601 (2020) 125047. https://doi.org/10.1016/j.colsurfa.2020.125047

[3] L. He, Y. Shi, Q. Wang, D. Chen, J. Shen, S. Guo, Strategy for constructing electromagnetic interference shielding and flame retarding synergistic network in poly (butylene succinate) and thermoplastic polyurethane multilayered composites, Composites Science and Technology 199 (2020) 108324. https://doi.org/10.1016/j.compscitech.2020.108324

[4] X. Zhang, Y. Xu, X. Zhang, H. Wu, J. Shen, R. Chen, Y. Xiong, J. Li, S. Guo, Progress on the layer-by-layer assembly of multilayered polymer composites: Strategy, structural control and applications, Progress in Polymer Science 89 (2019) 76–107. https://doi.org/10.1016/j.progpolymsci.2018.10.002

[5] Q. Huang, When Polymer Chains Are Highly Aligned: A Perspective on Extensional Rheology, Macromolecules 55 (2022) 715–727. https://doi.org/10.1021/acs.macromol.1c02262.

[6] F. Gholami, L. Pakzad, E. Behzadfar, Morphological, interfacial and rheological properties in multilayer polymers: A review, Polymer 208 (2020) 122950. https://doi.org/10.1016/j.polymer.2020.122950

[7] H. Zhang, K. Lamnawar, A. Maazouz, J.M. Maia, A nonlinear shear and elongation rheological study of interfacial failure in compatible bilayer systems, Journal of Rheology 60 (2016) 1–23. https://doi.org/10.1122/1.4926492

[8] B.H. Zimm, W.H. Stockmayer, The dimensions of chain molecules containing branches and rings, The Journal of Chemical Physics 17 (1949) 1301–1314. https://doi.org/10.1063/1.1747157

[9] D. Auhl, J. Stange, H. Münstedt, B. Krause, D. Voigt, A. Lederer, U. Lappan, K. Lunkwitz, Long-Chain Branched Polypropylenes by Electron Beam Irradiation and Their Rheological Properties, Macromolecules 37 (2004) 9465–9472. https://doi.org/10.1021/ma030579w

[10] J. Stange, C. Uhl, H. Münstedt, Rheological behavior of blends from a linear and a long-chain branched polypropylene, Journal of Rheology 49 (2005) 1059–1079. https://doi.org/10.1122/1.2008297

[11] M. Sugimoto, T. Tanaka, Y. Masubuchi, J.-I. Takimoto, K. Koyama, Effect of chain structure on the melt rheology of modified polypropylene, Journal of Applied Polymer Science 73 (1999) 1493–1500. https://doi.org/10.1002/(SICI)1097-4628(19990822)73:8<1493::AID-APP18>3.0.CO;2-2

[12] S. Kurzbeck, F. Oster, H. Münstedt, T.Q. Nguyen, R. Gensler, Rheological properties of two polypropylenes with different molecular structure, Journal of Rheology 43 (1999) 359–374. https://doi.org/10.1122/1.551040

[13] F.T. Trouton, On the coefficient of viscous traction and its relation to that of viscosity, Proceedings of the Royal Society of London. Series A, Containing Papers of a Mathematical and Physical Character 77 (1906) 426–440. https://doi.org/10.1098/rspa.1906.0038

[14] J.M. Dealy, D.J. Read, R.G. Larson, Structure and Rheology of Molten Polymers, in: J.M. Dealy, D.J. Read, R.G. Larson (Eds.), Structure and Rheology of Molten Polymers (Second Edition), Hanser, 2018: p. I–XVII. https://doi.org/10.3139/9781569906125.fm

[15] G. Liu, H. Sun, S. Rangou, K. Ntetsikas, A. Avgeropoulos, S.-Q. Wang, Studying the origin of "strain hardening": Basic difference between extension and shear, Journal of Rheology 57 (2013) 89–104. https://doi.org/10.1122/1.4763568

[16] M.H. Wagner, S. Kheirandish, M. Yamaguchi, Quantitative analysis of melt elongational behavior of LLDPE/LDPE blends, Rheologica Acta 44 (2004) 198–218. https://doi.org/10.1007/s00397-004-0400-9

[17] K. Hagita, H. Morita, M. Doi, H. Takano, Coarse-Grained Molecular Dynamics Simulation of Filled Polymer Nanocomposites under Uniaxial Elongation, Macromolecules 49 (2016) 1972–1983. https://doi.org/10.1021/acs.macromol.5b02799

[18] A. Huegun, M. Fernández, M.E. Muñoz, A. Santamaría, Rheological properties and electrical conductivity of irradiated MWCNT/PP nanocomposites, Composites Science and Technology 72 (2012) 1602–1607. https://doi.org/10.1016/j.compscitech.2012.06.011

[19] M. Hoseini, A. Haghtalab, M.H.N. Family, Elongational behavior of silica nanoparticle-filled low-density polyethylene/polylactic acid blends and their morphology, Rheologica Acta 59 (2020) 621–630. https://doi.org/10.1007/s00397-020-01225-5

[20] M. Kong, Y. Huang, Y. Lv, Q. Yang, G. Li, R.G. Larson, Elongation thinning and morphology deformation of nanoparticle-filled polypropylene/polystyrene blends in elongational flow, Journal of Rheology 62 (2018) 11–23. https://doi.org/10.1122/1.5009195

[21] B. Lu, P. Alcouffe, G. Sudre, S. Pruvost, A. Serghei, C. Liu, A. Maazouz, K. Lamnawar, Unveiling the Effects of In Situ Layer–Layer Interfacial Reaction in Multilayer Polymer Films via Multilayered Assembly: From Microlayers to Nanolayers, Macromolecular Materials and Engineering 305 (2020) 2000076. https://doi.org/10.1002/mame.202000076

[22] H. Zhang, K. Lamnawar, A. Maazouz, J.M. Maia, A nonlinear shear and elongation rheological study of interfacial failure in compatible bilayer systems, Journal of Rheology 60 (2016) 1–23. https://doi.org/10.1122/1.4926492

[23] B. Lu, K. Lamnawar, A. Maazouz, G. Sudre, Critical Role of Interfacial Diffusion and Diffuse Interphases Formed in Multi-Micro-/Nanolayered Polymer Films Based on Poly(vinylidene fluoride) and Poly(methyl methacrylate), ACS Appl. Mater. Interfaces 10 (2018) 29019–29037. https://doi.org/10.1021/acsami.8b09064

[24] L. Levitt, C.W. Macosko, T. Schweizer, J. Meissner, Extensional rheometry of polymer multilayers: A sensitive probe of interfaces, Journal of Rheology 41 (1997) 671–685. https://doi.org/10.1122/1.550829

[25] A. Dmochowska, J. Peixinho, C. Sollogoub, G. Miquelard-Garnier, Extensional Viscosity of Immiscible Polymer Multi-Nanolayer Films: Signature of the Interphase, Macromolecules 56 (2023) 6222–6231. https://doi.org/10.1021/acs.macromol.3c00288

[26] J. Li, A. Maazouz, K. Lamnawar, Unveiling the restricted mobility of carbon nanotubes inside a long chain branched polymer matrix via probing the shear flow effects on the rheological and electrical properties of the filled systems, Soft Matter 19 (2023) 9146–9165. https://doi.org/10.1039/D3SM01311A

[27] J. Wang, W. Yu, C. Zhou, Y. Guo, W. Zoetelief, P. Steeman, Elongational rheology of glass fiber-filled polymer composites, Rheologica Acta 55 (2016) 833–845. https://doi.org/10.1007/s00397-016-0960-5